Pergamon

Journal of Structural Geology, Vol. 18, No. 4, pp. 493 to 504, 1996

0191-8141/96 $15.00+0.00

0191-8141(95)00098-4

Balancing salt dome uplift and withdrawal basin subsidence in cross-section

ROGER C. BREWER*

Department of Geology, University of Alabama, Tuscaloosa, AL 35487, U.S.A.

and

PATRICIA M. KENYON

Department of Earth and Atmospheric Sciences, City College of New York, New York, NY 10031, U.S.A.

(Received 7 October 1992; accepted in revised form 6 June 1995)

Abstract—Idealized geometric models are presented for cases of cross-sections drawn perpendicular to elongate salt domes, where a two-dimensional model is adequate, and cross-sections drawn through the center of hemispherical salt domes, where a three-dimensional model is needed. Primary attention is devoted to domes during the salt pillow stage of uplift; however, a simple model is provided for the piercement stage as well. Mathematical relationships are derived between the cross-sectional area of the dome and the cross-sectional area of the associated withdrawal basin. Relationships are also derived relating non-dimensional dome uplift to non-dimensional basin subsidence. These relationships must be taken into account when constructing and restoring cross-sections of salt domes. Failure to do so can result in significant errors in estimating the amount of salt lost to dissolution. In addition, the relationships in this paper imply that there is a change in either salt dome height or withdrawal basin depth near the ends of an elongate dome, and predict that restored cross-sections of mini-basins developed on thick layers of salt typically will contain more salt than the present-day section.

INTRODUCTION

In recent years, there has been increased interest in balancing and restoring cross-sections of deformed strata above mobilized salt (e.g. Worrall & Snelson 1989). Doing this correctly requires a thorough understanding of the movement of the salt as well as deformation styles of the strata to be restored. Brewer (1991) discussed styles of domal uplifts in the strata overlying salt domes and presented techniques for the restoration and interpretation of such structures. Worrall & Snelson (1989) and Rowen (1993) described methods for restoring strata above mobilized salt taking into account such things as faulting, compaction and sediment deposition during deformation. In the latter papers, the salt is assumed to fill all areas not occupied by other lithologies. Sorenson (1986) discussed corrections which must be made to sediment volumes in withdrawal basins to account for remobilization of sediment during the rise of the diapir. To our knowledge, no work has been published that explicitly considers volume and area relationships for the salt itself in cross-section. The report presented here deals with this problem. Questions that will be addressed include: (1) 'What depth and width withdrawal basin is required to provide sufficient salt to form a given salt dome, assuming no dissolution of salt?'; (2) 'Under what circumstances can salt dome area and withdrawal basin area be assumed to be equal in cross-section?' and (3) 'How do these relationships change with variations in salt dome geometry?'.

The primary focus in this paper is on salt domes that have risen to a height less than their defining radius of curvature. Beyond this point, the salt dome passes from a 'pillow' stage to a 'piercement' stage and the continued growth of the withdrawal basin becomes complicated (Bishop 1978, Seni & Jackson 1983, Sorenson 1986). For mathematical convenience, salt pillows will be modeled geometrically by two end-member geometries; either as segments of spheres, having a height less than or equal to the radius of the sphere (hereafter called hemispherical domes), or elongate, flat-lying segments of cylinders with rounded ends (hereafter called elongate or anticlinal domes; Fig. 1). The shapes of real pillows in map view will lie somewhere between these end-members. Withdrawal basins associated with the pillows will be modeled as horizontal slices of doughnut or torus shapes surrounding a dome. It will be assumed that, in cross-section, both domes and basins are circular arcs defined by a fixed radius of curvature. An appendix defining the variables used in the equations is provided (Appendix A). Use of different shapes for the cross-sectional profiles would change the exact numbers for the relationships derived, but not the qualitative trends in the results.

Modifications of our calculations to describe a different geometric model for piercement diapirs are considered in the Discussion at the end of this paper. Qualitative agreement will be obtained between the

* Present address: 2417 Parker Place, Honolulu, HI 96822, U.S.A.

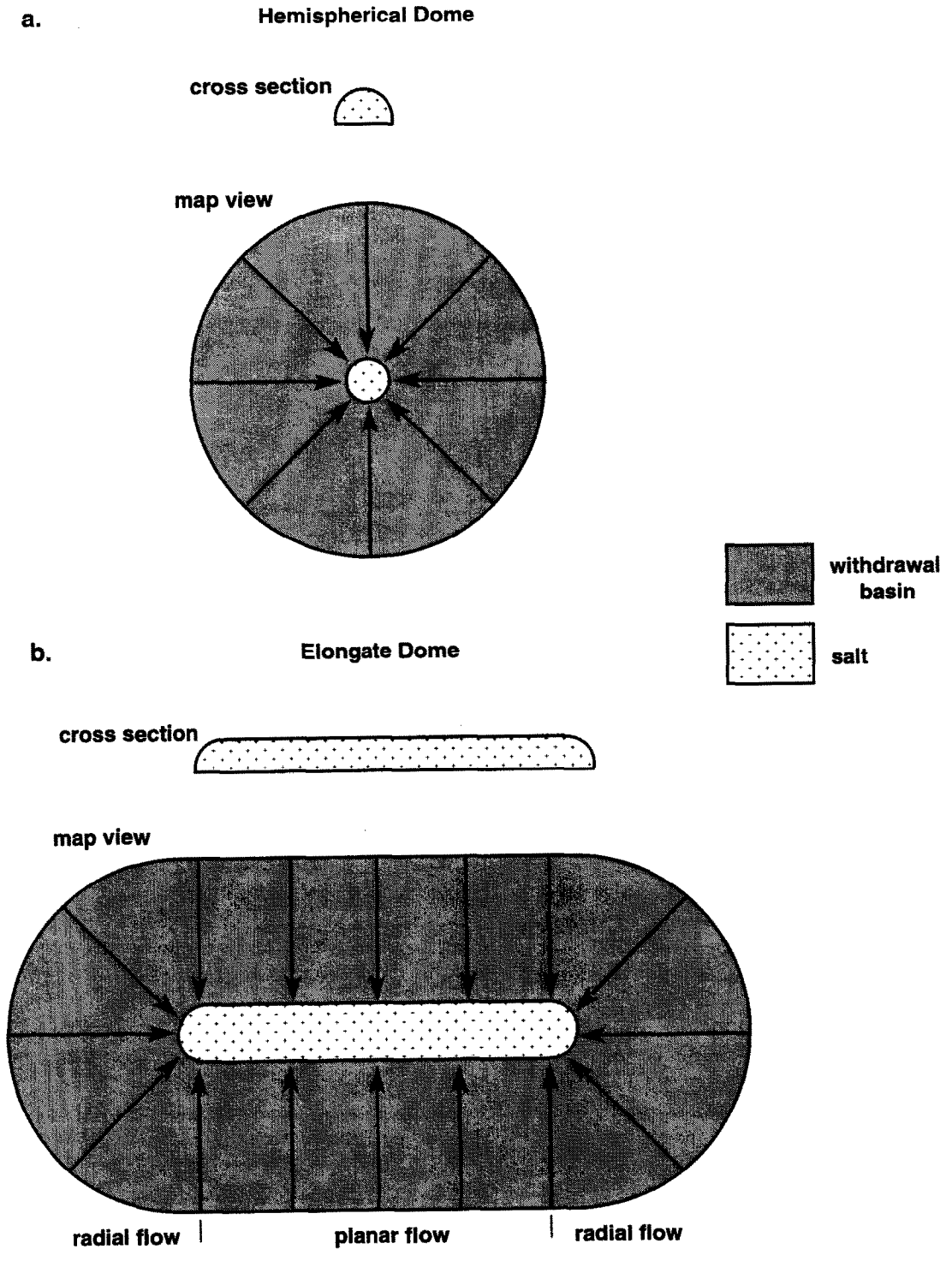

Fig. 1. Idealized salt dome geometries. The arrows in map view of withdrawal basin indicate the direction of salt flow. (a) Idealized hemispherical salt dome. (b) Idealized elongate salt dome.

calculations for the 'pillow' and 'piercement' stages of salt dome growth, suggesting that the qualitative results obtained are not critically dependent on the way in which the geometry is described mathematically.

Although simplified, the geometric models provide insight into the relationships between salt dome uplift, withdrawal basin subsidence and deformation of overburden. Calculations will be done for dome and withdrawal basin areas and volumes for both hemispherical and elongate domes. For salt pillows, graphs will be constructed to relate salt dome and withdrawal basin dimensions and areas during growth of the dome. Dimensions and areas will be those seen in a cross-section drawn perpendicular to the strike of an elongate dome in a location away from its ends and in a section drawn through the center of a hemispherical dome.

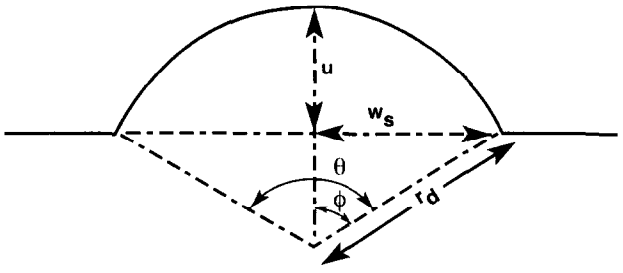

Fig. 2. Parameters used to define domes in cross-section: u = uplift, w_s = half-width of risen dome, r_d = radius of curvature defining arch, θ = angle defining sector, $\phi = \theta/2$.

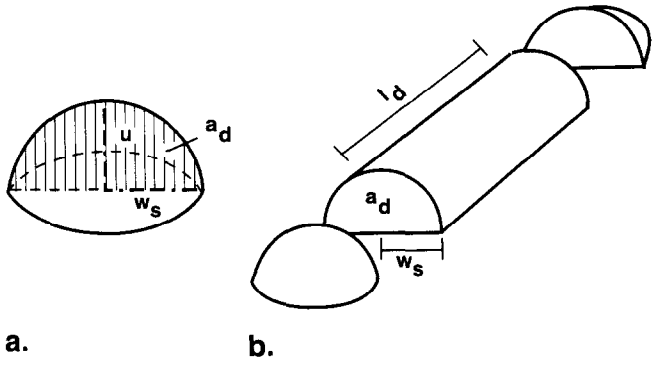

Fig. 3. (a) Parameters used to define hemispherical dome: u = uplift, w_s = half-width of dome, a_d = cross-sectional area of dome through its center. (b) Elongate dome: l_d = length of uplift minus rounded ends.

EQUATIONS DESCRIBING SALT DOMES AND WITHDRAWAL BASINS DURING THE PILLOW STAGE OF UPLIFT

Area of a dome in cross-section

A dome may be represented in cross-section as a portion of a circular arc (Fig. 2). The sector defined by the arc is composed of the dome and two right triangles of equal size. The total area of this sector is:

$$a_1 = \pi r_d^2 \frac{2\phi}{360} = \pi r_d^2 \frac{\phi}{180}, \tag{1}$$

where r_d is the radius of curvature of the arc defining the dome; and 2ϕ (or θ in Fig. 2) is the angle subtended by the sector in degrees.

The cross-sectional area, a_d, of the dome may be determined by subtracting the combined area, a_2, of the triangles from the total area, a_1, of the sector. By inspection of Fig. 2, the area of one of the triangles is:

$$a_2/2 = \frac{[(r_d - u)w_s]}{2}, \tag{2}$$

where u equals uplift of the dome and w_s equals the half-width of the dome.

Therefore, the cross-sectional area, a_d, of the dome is:

$$a_d = \pi r_d^2\left(\frac{\phi}{180}\right) - (r_d - u)w_s. \tag{3}$$

Expressing ϕ in terms of r_d and u produces:

$$a_d = \pi r_d^2 \frac{\cos^{-1}[1 - (u/r_d)]}{180} - (r_d - u)w_s. \tag{4}$$

In order to compare the areas of domes and withdrawal basins, it will be necessary to express equation (4) exclusively in terms of r_d and u. This can be done by using the Pythagorean theorem to relate w_s to r_d and u. The relationship is:

$$w_s = [2r_d u - u^2]^{1/2}. \tag{5}$$

Then, substituting (5) into (4) yields:

$$a_d = \pi r_d^2 \frac{\cos^{-1}[1 - (u/r_d)]}{180} - (r_d - u)[2r_d u - u^2]^{1/2}. \tag{6}$$

Alternatively, (4) can be expressed as a function of u and w_s. This is desirable in many applications, because, in nature, the dome uplift and width are the variables that can be directly measured. The radius of curvature, r_d, can be eliminated from the equations above by expressing it in terms of u and w_s as follows. Solving (5) for r_d produces:

$$r_d = (w_s^2 + u^2)/2u. \tag{7}$$

Then, substituting the expression for r_d from (7) into (4) and simplifying, we have:

$$a_d = \frac{\pi}{180}\left(\frac{w_s^2 + u^2}{2u}\right)^2 \cos^{-1}\left[1 - \frac{2u^2}{(w_s^2 + u^2)}\right] - \left[\left(\frac{w_s^2 + u^2}{2u}\right) - u\right]w_s, \tag{8}$$

giving an equation that describes the area of a dome in terms of the primary variables w_s and u.

Volume of dome

Idealized, three-dimensional shapes of domes are depicted in Fig. 3. The volume of a hemispherical dome can be taken directly from Eves (1985). It is:

$$v_{dh} = \frac{\pi}{6} u(3w_s^2 + u^2), \tag{9}$$

where u and w_s (Fig. 3a) are as defined above.

The volume of an elongate or anticlinal domal uplift can be calculated by summing the volume of the rounded ends and the volume of the elongate, middle section of the dome (Fig. 3b). The result is:

$$v_{de} = v_{dh} + l_d a_d. \tag{10}$$

Substituting the solution for v_{dh} from (9) and a_d from (8) into (10) produces the volume of an elongate dome in terms of the primary variables w_s and u:

$$v_{de} = \frac{\pi}{6} u(3w_s^2 + u^2) + l_d\left\{\frac{\pi}{180}\left(\frac{w_s^2 + u^2}{2u}\right)^2 \times \cos^{-1}\left[1 - \frac{2u^2}{(w_s^2 + u^2)}\right] - \left[\left(\frac{w_s^2 + u^2}{2u}\right) - u\right]w_s\right\}. \tag{11}$$

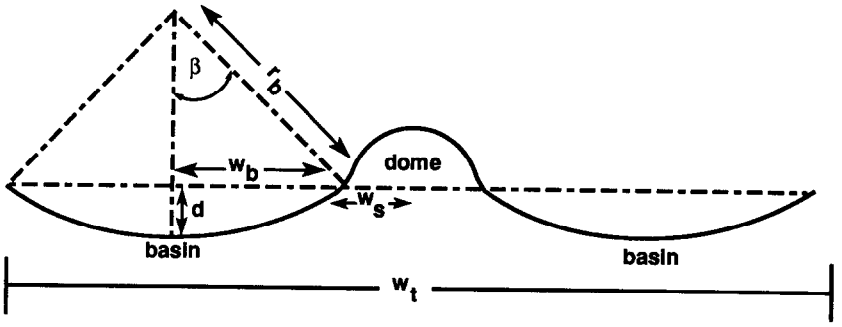

Fig. 4. Parameters used to define withdrawal basins in cross section: d = axial depth of basin, w_b = half-width of basin, r_b = radius of curvature defining basin, β = one-half of angle defining basin.

Area of withdrawal basin in cross-section

In cross-section, a withdrawal basin is modeled as a semi-circular depression (Fig. 4). The cross-sectional area of one side of the basin is calculated in a manner similar to that for a dome. Variables relating to the dome in equations (1)–(8) are replaced with the corresponding variables relating to the withdrawal basin (see Fig. 4). The radius of curvature, r_d, for the dome is replaced with the radius of curvature, r_b, defining the withdrawal basin. The angle ϕ for the dome is replaced with the angle β, half the angle of the sector defining the basin. Uplift, u, for the dome is replaced with depth, d, of the basin at its centerpoint. The half-width for the dome, w_s, is replaced with w_b, the half-width of one side of the basin.

The total area of the basin a_b in cross-section can then be calculated in terms of primary variables d and w_b by substituting w_b and d for w_s and u in the solution for a_d from (8) and multiplying the result by two (to include both sides of the basin). The result is:

$$a_b = 2\left\{\frac{\pi}{180}\left(\frac{w_b^2 + d^2}{2d}\right)^2 \cos^{-1}\left[1 - \frac{2d^2}{(w_b^2 + d^2)}\right] - \left[\left(\frac{w_b^2 + d^2}{2d}\right) - d\right]w_b\right\}. \quad (12)$$

Volume of withdrawal basin

Idealized geometric models of withdrawal basins are depicted in Fig. 5. The volume of a withdrawal basin associated with a hemispherical dome is expressed using the Pappus–Guldinus theorem for calculating the volume, v, of a solid of revolution (Eves 1985):

$$v = 2\pi R(a/2). \quad (13)$$

In this equation, it is assumed that a planar area, $a/2$ (one-half of the total area of the solid in cross-section), is revolved about an axis located a distance R from its center (Fig. 5a). The volume, v_{bh}, of the withdrawal basin associated with a hemispherical dome is calculated by substituting the length $w_b + w_s$ (the distance from the center of the dome to the center of the withdrawal basin) for R, and $a_b/2$ (the area of one side of the withdrawal basin) for $a/2$ in equation (13) (Fig. 5b). The result is:

$$v_{bh} = 2\pi(w_b + w_s)(a_b/2) = \pi(w_b + w_s)a_b. \quad (14)$$

The term w_s in the equation can be expressed in terms of w_b as follows. Based on physical models and study of natural salt domes, Parker & McDowell (1955) and Ramberg (1981) determined the average total width of the combined dome and withdrawal basin to be seven times the width of the dome itself. Restated, this means that one side of a withdrawal basin is approximately three times the width of the associated salt dome. The half-width of the withdrawal basin is therefore also three times the half-width of the dome (see Fig. 4), or:

$$w_b = 3w_s. \quad (15)$$

The use of a value other than three for w_b/w_s will produce a change in the numerical values calculated using the equations derived, but not in the qualitative trends visible in the results. Substituting (15) into (14) yields:

$$v_{bh} = \pi[w_b + (w_b/3)]a_b = \tfrac{4}{3}\pi w_b a_b. \quad (16)$$

Substituting the solution for a_b from (12) into (16) results in an equation for the volume of the basin associated with a hemispherical dome in terms of the primary variables w_b and d:

$$v_{bh} = \tfrac{8}{3}\pi w_b\left\{\frac{\pi}{180}\left(\frac{w_b^2 + d^2}{2d}\right)^2 \cos^{-1}\left[1 - \frac{2d^2}{(w_b^2 + d^2)}\right] - \left[\left(\frac{w_b^2 + d^2}{2d}\right) - d\right]w_b\right\}. \quad (17)$$

The volume, v_{be}, of the withdrawal basin associated with an elongate dome is equal to the volume of the rounded ends of the basin, calculated in the same manner as v_{bh} [equation (16)], plus the volume of the middle, trough-shaped parts of the basin (Fig. 5c). The total volume v_{be} of the elongate withdrawal basin is therefore:

$$v_{be} = v_{bh} + l_b a_b. \quad (18)$$

The volume of the withdrawal basin in terms of the primary variables w_b and d is obtained as follows. First, substituting for v_{bh} from (16) into (18) and rearranging, we obtain:

$$v_{be} = [\tfrac{4}{3}\pi w_b + l_b]a_b. \quad (19)$$

Then, substituting the solution for a_b from (12) into (19), we have:

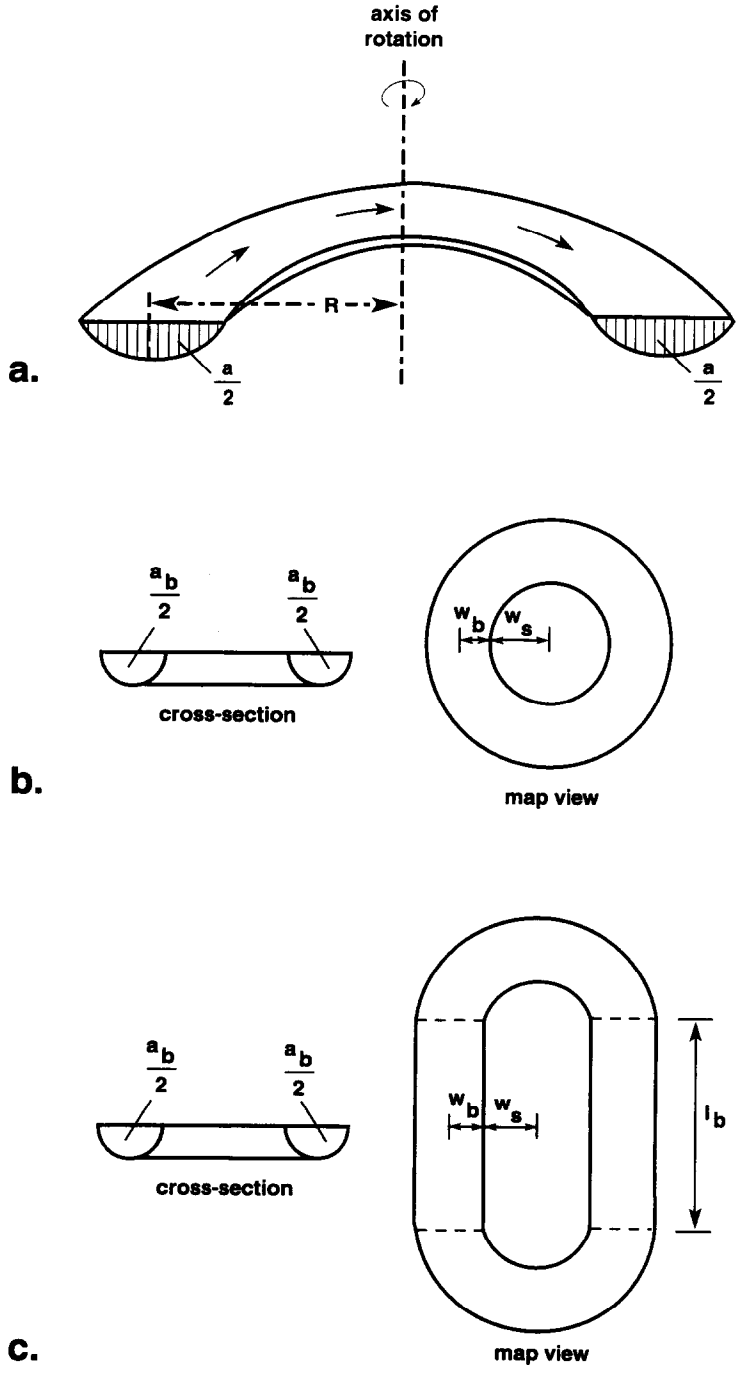

Fig. 5. (a) Half of a model withdrawal basin produced by rotating the cross-sectional area, $a/2$, 2π radians about a central axis. The center of the area is located a distance R from the axis of rotation. (b) Parameters of a withdrawal basin associated with a hemispherical dome: d = axial depth of basin, w_b = half-width of basin, w_s = half-width of dome, a_b = area of basin in cross-section. (c) Additional parameter for a withdrawal basin associated with an elongate dome: l_b = length of basin minus rounded ends.

$$v_{be} = 2\left[\tfrac{4}{3}\pi w_b + l_b\right]\left\{\frac{\pi}{180}\left(\frac{w_b^2 + d^2}{2d}\right)^2 \cos^{-1}\left[1 - \frac{2d^2}{(w_b^2 + d^2)}\right] - \left[\left(\frac{w_b^2 + d^2}{2d}\right) - d\right]w_b\right\}. \quad (20)$$

Equation (20) gives the volume of withdrawal basins associated with elongate domes in terms of the primary variables related to the basin. Use of a value other than three for w_b/w_s will change only the constant 4/3 in this equation.

BALANCING DOME AND BASIN AREA IN CROSS-SECTION

Elongate dome

The linear portion of an elongate salt dome is modeled as growing by planar flow of salt inward from the surrounding withdrawal basin perpendicular to the long axis of the anticline (see Fig. 1). Hemispherical domes and the rounded ends of elongate domes are modeled as

growing by radially convergent flow of salt inward from the surrounding withdrawal basin toward the center of the dome. As discussed later, with our assumption of hemispherical ends for an elongate dome, this produces a discontinuity in either the depth of the basin or the height of the dome near the ends. Barring loss of material to extrusion or dissolution, the volume of a withdrawal basin (the volume of the depression of the salt below the original salt top) should equal the volume of the associated dome in a cross-section perpendicular to the long axis of an elongate dome. Therefore, we can equate the area a_b of the withdrawal basin associated with a dome to the area a_d of the dome [equation (6)]. This gives:

$$a_b = a_d = \pi r_d^2 \frac{\cos^{-1}[1 - (u/r_d)]}{180} - (r_d - u)[2r_d u - u^2]^{1/2}. \quad (21)$$

Hemispherical dome

Balancing the cross-sectional area of a hemispherical dome and the area of the associated withdrawal basin is not so straightforward. Because salt moves radially in toward the dome, the area of the dome in cross-section will reflect out-of-plane contributions of salt. The area of the dome will, therefore, always be greater than the area of the basin viewed in the same cross-section for any given degree of uplift. This relationship will be quantified below by expressing the ratio of basin area to dome area as a function of the ratio of dome uplift to dome radius. First, to facilitate comparison with (6), basin area a_b is expressed in terms of r_d and u. Equating (9), the solution for the volume of a hemispherical dome, to (14), the solution for the volume of its associated withdrawal basin, produces:

$$\frac{\pi}{6} u(3w_s^2 + u^2) = \pi(w_b + w_s)a_b. \quad (22)$$

Solving for a_b, substituting $3w_s$ from (15) for w_b and rearranging yields:

$$a_b = \frac{u(3w_s^2 + u^2)}{24w_s}. \quad (23)$$

The area of the basin a_b can now be expressed in terms of r_d and u by substituting the solution for w_s from (5) into (23) and simplifying to get:

$$a_b = \frac{u}{24}\left[3(2r_d u - u^2)^{1/2} + \frac{u^2}{(2r_d u - u^2)^{1/2}}\right]. \quad (24)$$

Basin area is expressed as a fraction of dome area by dividing (24) by (6), the solution for dome area:

$$\frac{a_b}{a_d} = \frac{\frac{u}{24}\left[3(2r_d u - u^2)^{1/2} + \frac{u^2}{(2r_d u - u^2)^{1/2}}\right]}{\pi r_d^2 \frac{\cos^{-1}[1 - (u/r_d)]}{180} - (r_d - u)[2r_d u - u^2]^{1/2}}. \quad (25)$$

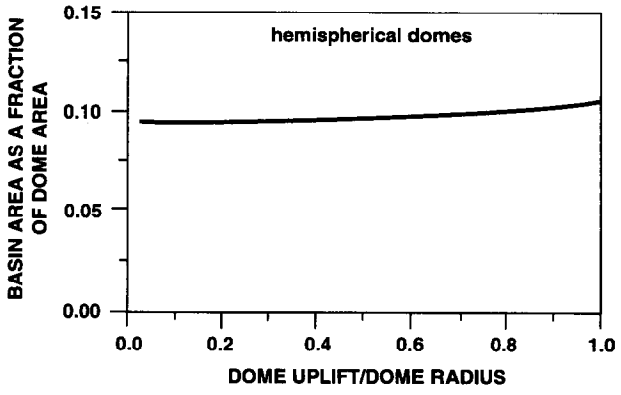

Fig. 6. Withdrawal basin area expressed as a fraction of dome area during uplift of a hemispherical dome defined by a fixed radius of curvature [equation (29)].

Multiplying the numerator and denominator of (25) by $1/r_d^2$ and simplifying produces:

$$\frac{a_b}{a_d} = \frac{\left[\frac{u}{24r_d}\right]\left\{3[2(u/r_d) - (u/r_d)^2]^{1/2} + \left\{\frac{u}{r_d}\right\}\left\{\frac{u/r_d}{[2(u/r_d) - (u/r_d)^2]^{1/2}}\right\}\right\}}{\frac{\pi}{180}\left\{\cos^{-1}[1 - (u/r_d)] - \left[1 - \frac{u}{r_d}\right][2(u/r_d) - (u/r_d)^2]^{1/2}\right\}}. \quad (26)$$

Equation (26) can be rewritten more simply by defining the non-dimensional uplift y, where:

$$y = u/r_d. \quad (27)$$

The non-dimensional uplift can be thought of as a measure of the shape of the salt pillow. Low y describes a salt pillow which is broad and low, while large y describes a pillow which is higher and narrower and is approaching the 'piercement' stage of salt dome evolution. In general, the equations derived in this section of this paper are valid only for $y < 1$. Substituting (27) into (26) and simplifying produces:

$$\frac{a_b}{a_d} = \frac{\frac{y}{24}\left[3(2y - y^2)^{1/2} + \frac{y^2}{(2y - y^2)^{1/2}}\right]}{\frac{\pi}{180}[\cos^{-1}(1 - y) - (1 - y)(2y - y^2)^{1/2}]}. \quad (28)$$

This equation can be further simplified by multiplying the numerator and denominator by $1/(2y - y^2)^{1/2}$. This produces the following equation for the ratio of basin area to dome area for a hemispherical dome in cross-section:

$$\frac{a_b}{a_d} = \frac{\frac{15y}{2\pi}\left[3 + \frac{y^2}{2y - y^2}\right]}{\frac{\cos^{-1}(1 - y)}{(2y - y^2)^{1/2}} - (1 - y)}. \quad (29)$$

The solution for (29) is plotted in Fig. 6. Inspection of that figure reveals that the cross-sectional area of the withdrawal basin associated with a hemispherical dome

is approximately an order of magnitude less than the cross-sectional area of the dome at any given stage of dome uplift. This is true despite the fact that the dome and withdrawal basin volumes are equal and contrasts with the one-to-one relationship between withdrawal basin area and dome area in the case of an elongate dome. It should be remembered that this result again pertains to a width ratio w_b/w_s of three. Use of a different ratio would change the constant 15/2 in (29). For example, if $w_b/w_s = 2$ were chosen, the constant would be 10, leading to a 33% larger value of a_b/a_d.

RELATIONSHIP BETWEEN BASIN SUBSIDENCE AND DOME UPLIFT

The equations for dome and basin area derived above can also be used to obtain equations relating basin subsidence, d, and dome uplift, u. The area of a withdrawal basin has been expressed in terms of variables relating directly to the basin itself (12) as well as in terms of variables relating only to the associated dome [equation (21) for elongate domes or equation (24) for hemispherical domes]. In Appendix B, (21) and (24) are each equated to (12) and transcendental equations are derived for withdrawal basin depth with respect to dome uplift. The final equations are:

$$\frac{\pi}{180}\cos^{-1}[1-y]-[1-y]\sqrt{2y-y^2} = \frac{\pi}{90}\left[\frac{9(2-y)+b^2y}{2b}\right]^2\cos^{-1}\left[1-\frac{2b^2y}{9(2-y)+b^2y}\right] - 6\left[\frac{9(2-y)+b^2y}{2b}-by\right]\sqrt{2y-y^2} \quad (30)$$

for an elongate basin, and:

$$\frac{y}{24}\left[3(2y-y^2)^{1/2}+\frac{y^2}{(2y-y^2)^{1/2}}\right] = \frac{\pi}{90}\left[\frac{9(2-y)+b^2y}{2b}\right]^2\cos^{-1}\left[1-\frac{2b^2y}{9(2-y)+b^2y}\right] - 6\left[\frac{9(2-y)+b^2y}{2b}-by\right]\sqrt{2y-y^2} \quad (31)$$

for a hemispherical one, where $b = d/u$ is the non-dimensional depth of the withdrawal basin.

These equations were solved for non-dimensional basin depth as a function of non-dimensional dome uplift by trial and error using a spreadsheet. Figure 7 shows the results for basin subsidence vs dome uplift for cases of both infinitely elongated domes (formed by purely planar flow of salt) and hemispherical domes (formed by purely radial flow of salt). In this case, several constants in the equation would change, if a different value of w_b/w_s were chosen; however, the qualitative result, that the withdrawal basins formed by purely planar flow of salt into a dome are significantly deeper than basins formed by radial flow of salt into a dome, would still be true.

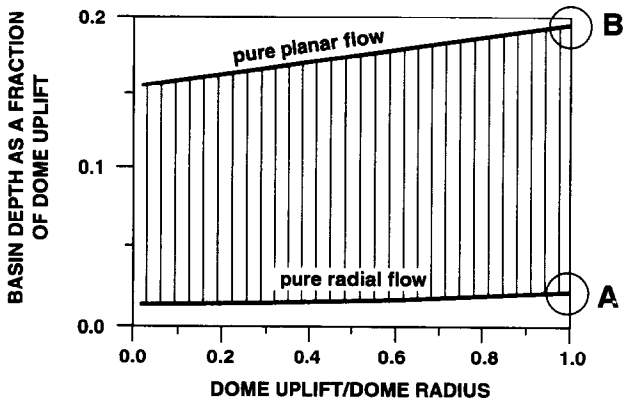

Fig. 7. Withdrawal basin depth expressed as a fraction of dome uplift during uplift of a hemispherical dome defined by a fixed radius of curvature. Low, broad pillows would lie toward the left side of this graph while higher, narrower pillows would lie toward the right. Depth is measured as subsidence along the axis of the basin trough. Upper curve represents basin depth in the idealized case of pure planar flow of salt into the mid-sections of infinitely elongate domes [determined by relating equation (12) to equation (21)]. Lower curve represents basin depth in the case of pure radial flow of salt into hemispherical domes or the rounded ends of elongate domes [determined by relating equation (12) to equation (25)]. Points 'A' and 'B' are the basin-depth-to-dome-uplift ratios for a dome-uplift-to-dome-radius ratio of one and are discussed in the text.

DISCUSSION

One use of the above equations for dome and withdrawal basin size and area is to predict the expected dimensions in cross-section for quantities associated with a salt dome of a particular size. Assume, for example, that a salt pillow in the shape of an idealized hemispherical dome with a height and radius of 1000 m forms from a layer of salt 800 m thick. (The thickness of the salt layer is not crucial for the argument which follows, as long as it is greater than the calculated depths of the withdrawal basins.) In cross-section, the dome would have an area of 1.6 km^2 [equation (6)]. The predicted total width of the withdrawal basin/dome system would be 14 000 m [i.e. $2(w_s + 2w_b)$, where w_b is given by equation (15)]. If the flow of salt into the dome is purely radial, the withdrawal basin would only have to subside approximately 20 m at its center line (two one-hundredths of the dome uplift, point A on Fig. 7) over an extent 6000 m wide [equation (15)] in order to yield a large enough volume of salt to build the dome. The withdrawal basin would thus constitute only a small perturbation on the thickness of the salt bed (Fig. 8). In cross-section, the basin would have an area of approximately 0.16 km^2, which equals one-tenth the area of the dome [equation (12)]. Now assume that purely planar flow of salt occurs to form the mid-section of an elongate dome of the same height and width. Subsidence of a withdrawal basin in this area would be approximately 200 m (two-tenths of the dome uplift, point B in Fig. 7). The dome and withdrawal basin areas for the elongate dome would be equal in cross-section and the thickness of the original salt layer would be reduced by 25%, as shown in Fig. 8. At the same time, assuming purely radial flow of salt into the rounded ends of the elongate

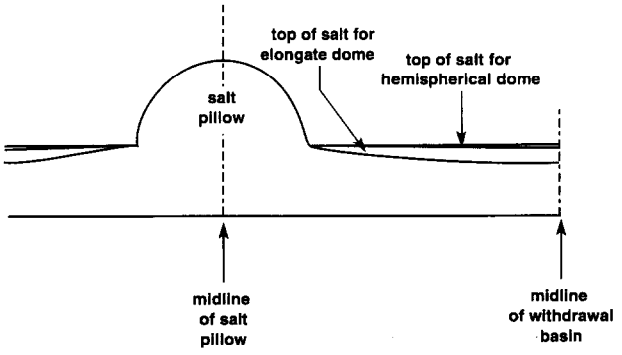

Fig. 8. Sketch showing withdrawal basin depths in cross-section for a hypothetical salt dome 1000 m in radius, assuming first hemispherical and then elongate geometry.

dome, subsidence of the withdrawal basin in these areas could be as little as 20 m. The contrast between the subsidence at the center and at the ends of an elongate dome is considerable and might lead one to think that no salt was contributed to the dome from the areas near its ends. Calculations of this type may prove useful for estimating the expected size of the withdrawal basin of a dome given the dimensions of the dome. A comparison between the expected size and that actually observed can be used as a check on kinematic models for formation of the dome formulated based on other evidence.

The relationships derived in this paper must also be taken into account when using cross-sections to estimate whether or not a given dome has lost significant amounts of salt due to extrusion and/or dissolution, based on the volume of strata in its withdrawal basin. Consider the cross-section in Fig. 8, showing the 1000 m dome described above with the 200 m deep withdrawal basin (the lower line in Fig. 8). If this is a cross-section taken perpendicular to the long axis of an elongate dome formed by planar flow of salt, then the observed depth of the basin is that expected when the basin and dome volumes are equal, and no salt has been lost to dissolution. However, if this is a cross-section across a hemispherical dome formed by radial flow, the basin volume will be significantly greater than the dome volume, and significant salt will have been lost. (If no salt had been lost, the basin floor would lie at the level of the upper line in Fig. 8.) We can estimate the volume of salt lost by the following calculation. From equation (9), the volume of the hemispherical dome is 2.09 km^3. From equation (17), the basin volume calculated, assuming radial flow into the dome, is 20.1 km^3. The difference is 18.0 km^3. In this case, one would conclude that a salt volume of approximately nine times the dome volume has been lost, presumably to dissolution. This shows the extreme sensitivity of volume balancing to the type of flow which created the dome, and it implies that estimation from cross-sections of the amount of salt lost during formation of a dome requires accurate knowledge of the amount of radial flow which has occurred.

The flow of salt into natural domes is probably never purely radial or linear. The curves in Fig. 7 therefore represent the maximum and minimum depths of idealized withdrawal basins, and there is probably a continuum between these two extremes. Near elongate domes, however, these extremes could exist in close proximity to one another. The discontinuity between subsidence due to radial flow of salt vs subsidence due to planar flow of salt could potentially create significant changes in withdrawal basin depth around the hemispherical ends of elongate salt domes, where salt flow changes from being planar to radial (refer to Fig. 1). Assuming the dome maintains a constant height along its length, the depth of the withdrawal basin adjacent to the rounded ends could be up to an order of magnitude less than the depth of the basin along the elongate flanks of the dome. As a result, this portion of the basin could be missed in studies of the volume balance between withdrawal basin sediments and mobilized salt. If, in contrast, the withdrawal basin were assumed to maintain a constant depth around the dome, the excess salt flowing into the ends could either redistribute itself equally throughout the dome or remain at the ends and lead to the growth of tall, secondary salt structures in these areas. Possible examples of the latter have been observed by one of the authors (R.C.B.) in confidential, unpublished seismic data from the Gulf of Mexico.

The concepts described in this paper will also apply in an inverse manner to small basins of clastic sediments developed over a thick layer of salt. Mini-basins of the foregoing type, developed by down-building, are characteristic of the Louisiana structural style of Worrall & Snelson (1989). If the assumptions of geometry made in the derivation of the equations in this paper are satisfied, these equations can be used to determine the expected area balance in cross-section between clastic sediments in the mini-basin and the displaced salt. All that is needed is to substitute the dimensions of the mini-basin for those of the salt dome and the dimensions of the displaced salt for those of the withdrawal basin in the equations. The equations show that, when a mini-basin is elongate in shape, it can be expected that the area occupied by the deposited strata and the area occupied by the displaced salt will be equal in a cross-section drawn perpendicular to the long axis of the basin. However, where such a basin is approximately equidimensional in map view, which is actually more common in offshore Louisiana, it can be expected that much of the displaced salt will be transported out of the plane of the cross-section. This will result in the amount of salt in a palinspasticaly restored cross-section being greater than that in the present-day section. This is quite common in sections in the central Louisiana offshore (Worrall & Snelson, 1989). The equations show that such an increase in salt area during restoration can exist without implying dissolution of salt or large-scale regional salt transport. The displaced salt from, for example, a 1 km deep hemispherical basin can be accommodated by a maximum increase of 20 m in the thickness of the salt layer surrounding the basin, an increase which is well within the range of possibility. This calculation shows that large-scale salt transport or dissolution is not necessary to explain the development of mini-basins.

Given the extreme sensitivity of the withdrawal basin (or in this case displaced salt) dimensions to the geometry of flow, however, predicting the detailed thickening of the salt layer which is expected for a particular mini-basin is probably best done in many cases by constructing a detailed volume balance specific to the geometry of each mini-basin.

As stated in the Introduction, the above relationships have all been developed for the salt pillow stage of salt dome growth. Here we would like to discuss the extension of the same reasoning to the piercement stage of salt dome growth. Emplacement of piercement diapirs is discussed by Bishop (1978) and Seni & Jackson (1983). As a salt dome enters this stage, it develops an accompanying secondary rim syncline which is narrower with respect to dome width than the primary rim syncline developed during the pillow stage. Consequently, the first modification which must be made in our theory is to substitute a different equation for (15) above. Examination of a number of structural contour maps of salt domes and their secondary peripheral sinks suggests that w_b is approximately equal to $2w_s$ for many domes. The second modification which must be made has to do with the shape of the salt dome, which is now closer to a tall column of salt than a hemispherical cap or a cylindrical cap with rounded ends. As a first approximation, we can assume that an equi-dimensional piercement dome (axisymmetric dome) has the shape of a vertical cylinder with flat ends and an elongate piercement dome (salt wall) has the shape of a vertical sheet with a flat top and rounded ends (Fig. 9). In that case, we can immediately write down equations, equivalent to (8), (9) and (11) for salt pillows, by inspection of Figs. 9 and 10, as follows:

$$\text{area of dome in cross-section} = (a_d)_p = 2w_s u \tag{32}$$

$$\text{volume of axisymmetric dome} = (V_{dh})_p = \pi w_s^2 u \tag{33}$$

$$\text{volume of salt wall} = (V_{de})_p = \pi w_s^2 u + 2u w_s l_d, \tag{34}$$

where u, w_s and l_d have the same definitions as they had for salt pillows, and the subscript 'p' indicates 'piercement'.

Note that the height u of the dome as defined here does not include the depth h of the withdrawal basin (Fig. 10). This is because the salt in the dome below the top of the withdrawal basin is replacing salt originally in that position in the salt layer. As a result, the total apparent height of the salt dome in cross-section will be $(u + h)$. The shapes of the withdrawal basins surrounding piercement salt domes are often complex. As a first approximation, we will assume that the basins have a wedge shape, with their deepest point h adjacent to the dome (Figs. 9 and 10). We will further assume that the basins completely surround the domes. With these assumptions, the area of the basin in a cross-section across the center of the axisymmetric dome or perpendicular to the strike of the salt wall (including both sides of the basin) is:

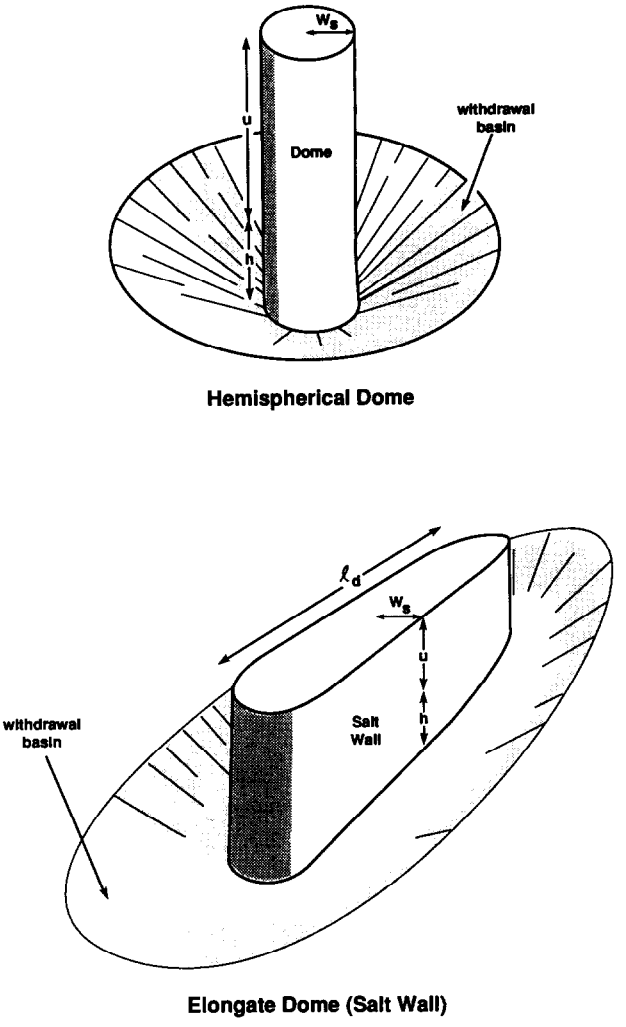

Fig. 9. Idealized geometries for piercement salt domes.

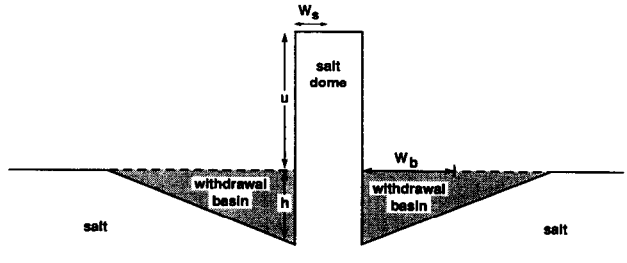

Fig. 10. Idealized cross-section of a piercement salt dome and its associated withdrawal basin. Cross-section is assumed to be taken across the center of a cylindrical dome or perpendicular to the strike of a salt wall. The height of the salt dome above the original top of the salt layer is denoted by u and the maximum depth of the withdrawal basin by h; w_s and w_b are the half-widths of the dome and the withdrawal basin, respectively.

$$(a_b)_p = 2w_b h. \tag{35}$$

For the axisymmetric dome, the volume of the withdrawal basin can be found by substituting $w_b h$ for a and $(w_b + w_s)$ for R in (13). The result is:

$$(v_{bh})_p = \pi(w_b + w_s)(w_b h), \tag{36}$$

and substituting $w_s = w_b/2$ into (36), we get:

$$(v_{bh})_p = \frac{3\pi}{2} w_b^2 h. \tag{37}$$

Finally, for the salt wall, substitution of $(v_{bh})_p$ for v_{bh}, $(a_b)_p$ for a_b and l_d for l_b in (18) yields:

$$(V_{be})_p = \frac{3\pi}{2} w_b^2 h + 2 w_b h l_d. \tag{38}$$

We now have all the equations we need to generate comparisons of dome and basin areas and depths analogous to those for salt pillows.

Basin subsidence can be compared with dome uplift for axisymmetric domes by equating (33) and (37). Doing this and rearranging, we obtain:

$$\frac{h}{u} = \frac{2}{3} \frac{w_s^2}{w_b^2}. \tag{39}$$

If we let $w_b = c w_s$, where c is some constant, then (39) becomes:

$$\frac{h}{u} = \frac{2}{3c^2}. \tag{40}$$

This means that the ratio of basin subsidence to dome uplift for an axisymmetric dome depends only on the relative widths of the dome and the basin. For our assumed value of $c = 2$ for piercement salt domes, this ratio comes out as 1/6, which is larger than in the pillow case, in accordance with observations.

The ratio of basin subsidence to dome uplift can be calculated for salt walls by equating (34) and (38). After rearranging, the result is

$$\frac{h}{u} = \frac{\pi w_s^2 + 2 w_s l_d}{\frac{3\pi}{2} w_b^2 + 2 w_b l_d}. \tag{41}$$

Substituting $w_b = c w_s$ into (41) and simplifying produces:

$$\frac{h}{u} = \frac{\pi w_s + 2 l_d}{\frac{3\pi}{2} c^2 w_s + 2 c l_d}, \tag{42}$$

which depends only on the dimensions of the dome and the basin. For very long domes ($l_d \gg w_s$), the terms containing w_s can be neglected and (41) reduces further to:

$$\frac{h}{u} = \frac{1}{c}, \tag{43}$$

which again depends only on the width of the withdrawal basin relative to the dome. For $c = 2$, equation (43) predicts a ratio of 1/2, again greater than that for a salt pillow.

Finally, for dome and basin area, we again have that the areas for an elongate dome (salt wall) are equal in a cross-section taken perpendicular to strike. For an axisymmetric dome, we can take the ratio of (32) and (35) to obtain:

$$\frac{(a_d)_p}{(a_b)_p} = \frac{w_s u}{w_b h}. \tag{44}$$

Substituting $w_b = c w_s$ into (44) produces:

$$\frac{(a_d)_p}{(a_b)_p} = \frac{1}{c} \frac{u}{h}. \tag{45}$$

Finally, substituting (40) into (45), we have:

$$\frac{(a_d)_p}{(a_b)_p} = \frac{3c}{2}, \tag{46}$$

which yields a ratio of three using our assumed value of 2 for c. Thus, the area of the piercement salt dome in cross-section will be three times the area of the associated withdrawal basin.

Finding an unequivocal field example of the principles discussed in this paper is difficult. Most seismic data is proprietary, and seismic sections of salt domes which have been published rarely extend far enough away from the dome to show the whole withdrawal basin. Nevertheless, one relatively clear example can be found in a pair of sections published in Jenyon (1986). These sections are shown in Fig. 11. The sections cross two salt domes from the same area of the North Sea, one an axisymmetric piercement dome and one a salt wall. They clearly show a larger withdrawal basin associated with the salt wall than with the axisymmetric dome. This was interpreted by Jenyon as due to the timing of formation of the two features, but it can also be explained by the principles discussed in this paper.

SUMMARY AND CONCLUSIONS

In this paper, salt domes in the pillow stage are geometrically modeled as idealized axisymmetric hemispheres and elongate cylindrical caps, and their associated withdrawal basins are modeled as slices through torus shapes. Balancing dome and withdrawal basin volumes and areas for salt pillows shows that primary withdrawal basins (assumed to be seven times the width of the dome) in cross-section are very shallow, as shallow as 2% of the dome height in the case of hemispherical domes. Such basins may not be resolvable on seismic lines if the dome has risen no higher than its defining radius of curvature. The areas of a dome and its associated withdrawal basin will be equal in a cross-section taken perpendicular to the strike of an elongate dome; however, for a hemispherical dome, the area of the dome will be significantly greater than that of the basin.

The results derived here predict a discontinuity near the ends of an elongate dome in either the height of the dome or the depth of its withdrawal basin. Also, application of the results to a hypothetical salt dome show that conclusions regarding the volume of salt lost to dissolution are extremely sensitive to the geometry of the salt flow forming the dome. Finally, application of the results to basins of clastic sediment developed over

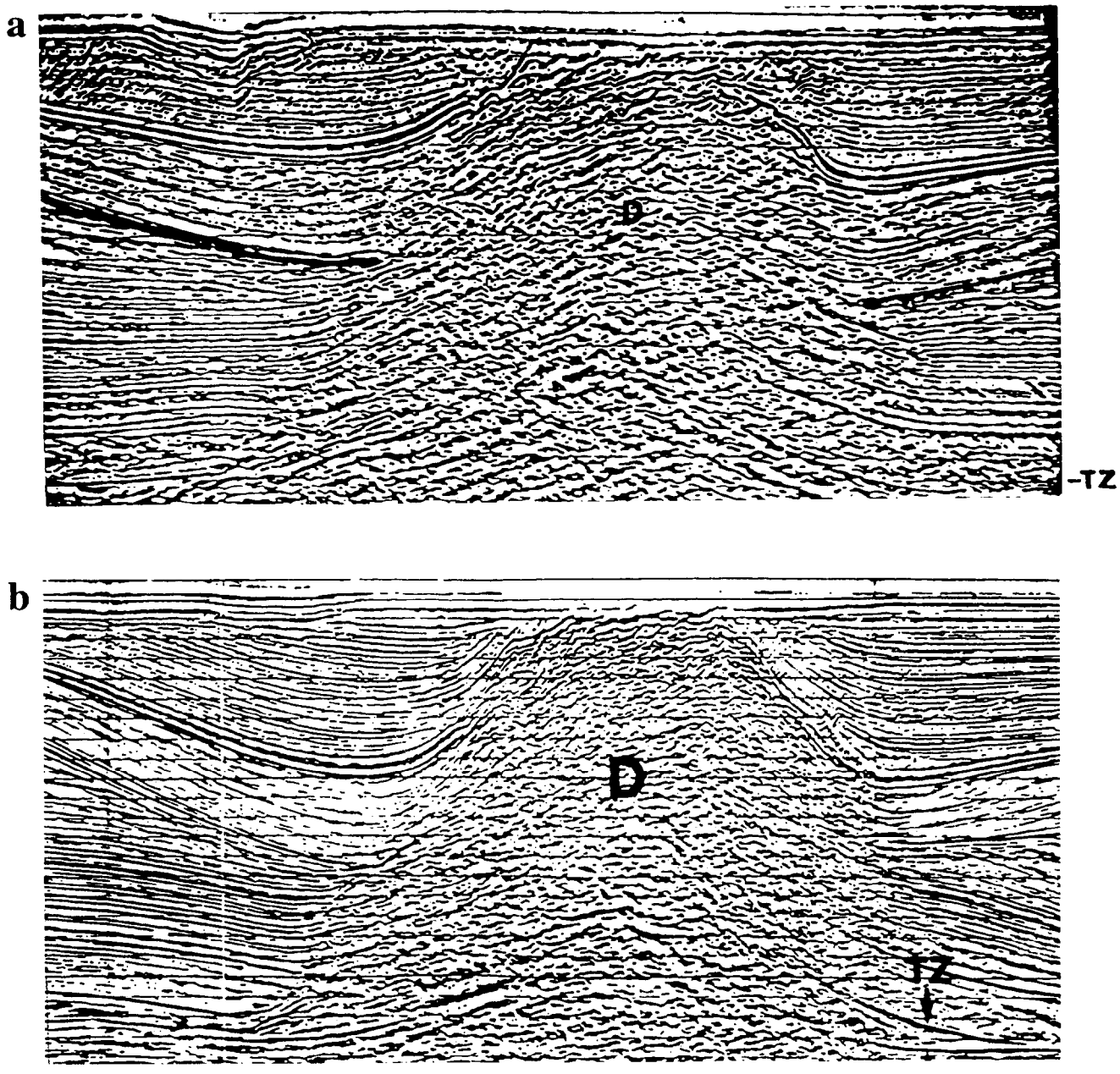

Fig. 11. Portions of seismic sections for a pair of salt structures from the Southern North Sea. These sections were originally published in Jenyon (1986, pp. 134–136) and are used by permission of Chapman and Hall. (a) Axisymmetric piercement diapir. (b) Salt wall. In these sections, D denotes the location of the diapir, and the TZ is the top of the salt layer.

thick beds of salt suggest that out-of-plane motion of salt can account for the common result that the amount of salt in a palinspastically restored cross-section is greater than that in the present-day section.

Results analogous to those for salt pillows are also derived for a simple geometrical model of piercement diapirs. These show, in agreement with observations, that the areas of domes and basins in cross-section and the depths of dome uplift and withdrawal basin subsidence are typically more nearly equal than they are in the salt pillow stage of dome growth; however, there is still a difference in cross-sectional area between dome and basin for the axisymmetric dome. Also, the depth of the withdrawal basin for an axisymmetric dome is still less than that for a salt wall of the same height and cross-sectional area.

Acknowledgements—Critical reviews of earlier drafts of the paper by Richard H. Groshong Jr, Christopher J. Talbot and an anonymous reviewer greatly assisted in improving the clarity of the text. The research was supported in part by grants from the Mobil Foundation (to R. H. G.) and Sigma Xi (to R. C. B.). The final two years of research were conducted under a Graduate Council Research Fellowship provided to R. C. B. by the University of Alabama Graduate School.

REFERENCES

Bishop, R. S. 1978. Mechanism for emplacement of piercement diapirs. *Am. Ass. Petrol. Geol. Bull.* **62**, 1561–1583.

Brewer, R. C. 1991. Structural patterns and strain distributions above domal uplifts. Unpublished Ph.D. thesis, University of Alabama, Tuscaloosa, Alabama.

Eves, H. 1985. Mensuration formulas. In: *CRC Standard Mathemat-*

ical Tables (27th edn; Beyer, W. H., editor). CRC Press, Boca Raton, Florida, 121–133.
Jenyon, M. K. 1986. *Salt Tectonics*. Elsevier Applied Science, London.
Parker, T. J. & McDowell, A. N. 1955. Model studies of salt dome tectonics. *Am. Ass. Petrol. Geol. Bull.* **39**, 2384–2470.
Ramberg, H. 1981. *Gravity, Deformation and the Earth's Crust in Theory, Experiments and Geological Applications* (2nd edn). Academic Press, London.
Rowen, M. G. 1993. A systematic technique for the sequential restoration of salt structures. *Tectonophysics* **228**, 331–348.
Seni, S. J. & Jackson, M. P. A. 1983. Evolution of salt structures, East Texas Diapir Province, part 1: sedimentary record of halokinesis. *Am. Ass. Petrol. Geol. Bull.* **67**, 1219–1244.
Sorenson, K. 1986. Rim syncline volume estimation and salt diapirism. *Nature* **319**, 23–27.
Worrall, D. M. & Snelson, S. 1989. Evolution of the northern Gulf of Mexico, with emphasis on Cenozoic growth faulting and the role of salt. In: *The Geology of North America—An Overview* (edited by Bally, A. W. & Palmer, A. R.). Geological Society of America, Boulder, 97–138.

APPENDIX A

List of variables

a_1	Total area of sector
a_2	Area of portion of sector below the dome
a_b	Cross-sectional area of withdrawal basin through dome crest
a_d	Cross-sectional area of dome through crest
b	Non-dimensional basin subsidence (d/u)
c	Ratio of half-width of withdrawal basin to half-width of dome
d	Depth of withdrawal basin at trough
h	Depth of withdrawal basin for piercement dome
l_b	Length of withdrawal basin minus rounded ends
l_d	Length of elongate dome minus rounded ends
R	Distance from midpoint of solid ring to center of axis of symmetry
r_d	Radius of curvature defining dome
r_b	Radius of curvature defining withdrawal basin
u	Uplift of dome above original top of salt layer
v	Volume of torus
v_{be}	Volume of withdrawal basin associated with an elongate dome
v_{bh}	Volume of withdrawal basin associated with a hemispherical dome
v_{bm}	Volume of middle section of elongate withdrawal basin
v_{de}	Volume of elongate dome
v_{dh}	Volume of hemispherical dome
v_{dm}	Volume of middle section of elongate dome
w_b	Half-width of withdrawal basin
w_s	Half-width of dome
w_t	Total width of withdrawal basin
y	Non-dimensional dome uplift (u/r_d)
β	One-half of angle defining withdrawal basin
θ	Angle defining sector of circle
ϕ	$\theta/2$

APPENDIX B

This appendix gives the details of the derivation of the relationship between non-dimensional basin subsidence and non-dimensional dome uplift for elongate and for hemispherical domes.

Consider first the elongate dome. Equation (21), which gives the area of the withdrawal basin for such a dome, can be rewritten in terms of the non-dimensional variable y, in the form:

$$a_b = r_d^2\left\{\frac{\pi}{180}\cos^{-1}\left[1-\frac{u}{r_d}\right]-\left[1-\frac{u}{r_d}\right]\left[2\frac{u}{r_d}-\frac{u^2}{r_d^2}\right]^{1/2}\right\}$$
$$= r_d^2\left\{\frac{\pi}{180}\cos^{-1}[1-y]-[1-y][2y-y^2]^{1/2}\right\}. \quad \text{(A1)}$$

Also, substituting the expression for w_b from (15) into (12) yields:

$$a_b = 2\left\{\frac{\pi}{180}\left[\frac{(3w_s)^2+d^2}{2d}\right]^2\cos^{-1}\left[1-\frac{2d^2}{(3w_s)^2+d^2}\right]\right.$$
$$\left.-\left[\frac{(3w_s)^2+d^2}{2d}-d\right]3w_s\right\}. \quad \text{(A2)}$$

Then, substituting the expression for w_s from (5) into (A2), we obtain:

$$a_b = 2\left\{\frac{\pi}{180}\left[\frac{9(2r_du-u^2)+d^2}{2d}\right]^2\cos^{-1}\left[1-\frac{2d^2}{9(2r_du-u^2)+d^2}\right]\right.$$
$$\left.-\left[\frac{9(2r_du-u^2)+d^2}{2d}-d\right]3[2r_du-u^2]^{1/2}\right\}. \quad \text{(A3)}$$

The arccosine term in (A3) can be simplified by multiplying numerator and denominator by u^{-2}, and a factor of u^2 can be pulled out of each of the other terms to get:

$$a_b = 2u^2\left\{\frac{\pi}{180}\left[\frac{u^{-2}[9(2r_du-u^2)+d^2]}{2u^{-1}d}\right]^2\cos^{-1}\left[1-\frac{2(d^2/u^2)}{9(2r_du^{-1}-1)+d^2u^{-2}}\right]\right.$$
$$\left.-3\frac{1}{u}\left[\frac{9(2r_du-u^2)+d^2}{2d}-d\right]\frac{1}{u}[2r_du-u^2]^{1/2}\right\}. \quad \text{(A4)}$$

This can be rewritten as:

$$a_b = 2u^2\left\{\frac{\pi}{180}\left[\frac{9\left(2\frac{r_d}{u}-1\right)+\frac{d^2}{u^2}}{2\frac{d}{u}}\right]^2\cos^{-1}\left[1-\frac{2\left(\frac{d^2}{u^2}\right)}{9\left(2\frac{r_d}{u}-1\right)+\frac{d^2}{u^2}}\right]\right.$$
$$\left.-3\left[\frac{9\left(2\frac{r_d}{u}-1\right)+\frac{d^2}{u^2}}{2\frac{d}{u}}-\frac{d}{u}\right]\left[2\frac{r_d}{u}-1\right]^{1/2}\right\}. \quad \text{(A5)}$$

Letting $y = u/r_d$ and $b = d/u$, (A5) reduces to:

$$a_b = 2u^2\left\{\frac{\pi}{180}\left[\frac{9(2y^{-1}-1)+b^2}{2b}\right]^2\cos^{-1}\left[1-\frac{2b^2}{9(2y^{-1}-1)+b^2}\right]\right.$$
$$\left.-3\left[\frac{9(2y^{-1}-1)+b^2}{2b}-b\right]\sqrt{2y^{-1}-1}\right\}. \quad \text{(A6)}$$

Equating (A1) to (A6) produces our final equation relating b and y for an elongate diapir. This equation is:

$$\frac{\pi}{180}\cos^{-1}[1-y]-[1-y]\sqrt{2y-y^2}$$
$$= 2y^2\left\{\frac{\pi}{180}\left[\frac{9(2y^{-1}-1)+b^2}{2b}\right]^2\cos^{-1}\left[1-\frac{2b^2}{9(2y^{-1}-1)+b^2}\right]\right.$$
$$\left.-3\left[\frac{9(2y^{-1}-1)+b^2}{2b}-b\right]\sqrt{2y^{-1}-1}\right\} \quad \text{(A7)}$$

or, simplifying:

$$\frac{\pi}{180}\cos^{-1}[1-y]-[1-y]\sqrt{2y-y^2}$$
$$= \frac{\pi}{90}\left[\frac{9(2-y)+b^2y}{2b}\right]^2\cos^{-1}\left[1-\frac{2b^2y}{9(2-y)+b^2y}\right]$$
$$-6\left[\frac{9(2-y)+b^2y}{2b}-by\right]\sqrt{2y-y^2}. \quad \text{(A8)}$$

For a hemispherical diapir, we must use equation (24) from the main text in place of equation (21) [i.e. eqn. (A1)]. Equation (24) can be rewritten as:

$$a_b = r_d^2\left(\frac{u}{24r_d}\right)\left[3\left(2\frac{u}{r_d}-\frac{u^2}{r_d^2}\right)^{1/2}+\frac{(u/r_d)^2}{\left(2\frac{u}{r_d}-\frac{u^2}{r_d^2}\right)^{1/2}}\right] \quad \text{(A9)}$$

and, substituting in $y = u/r_d$, this becomes:

$$a_b = r_d^2\left(\frac{y}{24}\right)\left[3(2y-y^2)^{1/2}+\frac{y^2}{(2y-y^2)^{1/2}}\right]. \quad \text{(A10)}$$

Finally, equating (A10) to (A6) and simplifying produces:

$$\frac{y}{24}\left[3(2y-y^2)^{1/2}+\frac{y^2}{(2y-y^2)^{1/2}}\right]$$
$$= \frac{\pi}{90}\left[\frac{9(2-y)+b^2y}{2b}\right]^2\cos^{-1}\left[1-\frac{2b^2y}{9(2-y)+b^2y}\right]$$
$$-6\left[\frac{9(2-y)+b^2y}{2b}-by\right]\sqrt{2y-y^2}. \quad \text{(A11)}$$